Research paper

On the azimuth angle characteristics of the blast wave from an underground magazine model (II)-Numerical simulation of a magazine with a small internal length-to-diameter ratio

Yuta Sugiyama†, Kunihiko Wakabayashi, Tomoharu Matsumura, and Yoshio Nakayama

National Institute of Advanced Industrial Science and Technology (AIST),
Central 5, 1-1-1 Higashi, Tsukuba, Ibaraki 305-8565, JAPAN
Phone : +81-29-861-0552
†Corresponding author : yuta.sugiyama@aist.go.jp

Received : November 28, 2016 Accepted : March 10, 2017

Abstract

We performed numerical simulations that modeled experiments in the previous paper (I) on a small-scale explosion inside an underground magazine both with and without a protective dike near the exit. The internal length-to-diameter ratio of the magazine was 3. To understand the effects of the dike on the azimuthal characteristics of the blast wave from the exit, the flow fields were visualized and the peak overpressure of the blast wave was measured. The azimuthal characteristics in the present simulations and the experiments showed good agreement. The dike prevented the detonation products from expanding along the exit direction and mitigates the peak overpressure near the dike. Incrementing the azimuth angle reduced the peak overpressure. The blast wave reflected off the dike, resulting in an enhanced blast wave behind the underground magazine. Our study showed that the iso-pressure circle in the case of a surface explosion would be converted into an iso-pressure ellipse in the case of an explosion from the underground magazine.

Keywords : numerical simulation, blast wave, azimuthal characteristics, dike effect, underground magazine

1. Introduction

In Japan, underground (tunnel-type) magazines are covered by regulations specifying that the explosive safety quantity-distance (ESQD) should be secured and is determined by the distance between the outside wall of the underground magazine to the residential area. Moreover, a dike should be located ahead of the exit to minimize the effects of any blast wave and fragments. However, in case of a detonation in an underground magazine, the shock wave would propagate inside the magazine and exit via the opening as a blast wave.

Skjeltorp et al.[1] studied the azimuthal characteristics of such a blast wave and proposed empirical equations in which the attenuation index of the peak overpressure versus the scaled distance is constant for all azimuth angles. This assumption is used in the safety standards of the Department of Defense Explosives Safety Board (DDESB)[2,3]. The blast-wave strength exhibited azimuthal characteristics in which the highest peak overpressure was along the exit direction and the lowest was behind the magazine. When a dike was situated at the exit, the reflection and diffraction at the dike disturbed the blast wave and changed the azimuthal characteristics[4]. This may result in a shorter ESQD behind the magazine exit and a longer one ahead of it.

In a previous study[4], we conducted small-scale experimental explosions both with and without a dike to determine the azimuthal characteristics of the blast wave from a model underground magazine with an internal length-to-diameter ratio $L/D = 3$. The dike both reflected and diffracted the blast wave ; the reflection enhanced the blast wave behind the magazine whereas the diffraction weakened it ahead of the magazine near the dike. The geometrical irregularity of the model cover induced a local

enhancement of the blast wave around 180°.

In this present study, we conduct numerical simulations of blast-wave propagation around a small-scale underground magazine to clarify the differences in azimuthal characteristics with and without a dike, and the effect of the dike on the propagation.

2. Numerical setup

We developed a multicomponent method[5] for two fluids based on the five-equation model proposed by Allaire et al.[5] In the present study, we use two fluids to reproduce our previous experiments[4]. The governing equations used here are the three-dimensional compressible Euler equations (Equation(1)) and a volume-fraction transport equation for the two fluids (Equation (2)).

$$\frac{\partial \mathbf{Q}}{\partial t}+\frac{\partial \mathbf{E}}{\partial x}+\frac{\partial \mathbf{F}}{\partial y}+\frac{\partial \mathbf{G}}{\partial z}=\mathbf{0}, \tag{1}$$

where

$$\mathbf{Q}=\begin{bmatrix}\alpha_1\rho_1\\ \alpha_2\rho_2\\ \rho v\\ \rho w\\ \rho e\end{bmatrix}, \mathbf{E}=\begin{bmatrix}\alpha_1\rho_1 u\\ \alpha_2\rho_2 u\\ \rho u^2+p\\ \rho vu\\ \rho wu\\ (\rho e+p)u\end{bmatrix}, \mathbf{F}=\begin{bmatrix}\alpha_1\rho_1 v\\ \alpha_2\rho_2 v\\ \rho uv\\ \rho v^2+p\\ \rho wv\\ (\rho e+p)v\end{bmatrix}, \mathbf{G}=\begin{bmatrix}\alpha_1\rho_1 w\\ \alpha_2\rho_2 w\\ \rho uw\\ \rho vw\\ \rho w^2+p\\ (\rho e+p)w\end{bmatrix},$$

$$\frac{\partial}{\partial t}(\alpha_1)+u\frac{\partial}{\partial x}(\alpha_1)+v\frac{\partial}{\partial y}(\alpha_1)+w\frac{\partial}{\partial z}(\alpha_1)=0. \tag{2}$$

Here, α_i and ρ_i indicate the volume fraction and density, respectively, of the i^{th} fluid ($i = 1$ for air, 2 for detonation products), u, v, and w are the velocities in the x, y, and z directions, respectively, p is the pressure, and e is the total energy per unit mass.

The ideal gas and Jones-Wilkins-Lee (JWL) equations of state (Equations (3) and (4)) are used to model the air and the detonation products, respectively, where ε_i indicates the internal energy per unit mass of the i^{th} fluid. The constitutive relationships are given in Equation (5). The pressure p of the multicomponent flow is calculated using the variables in Equations (1) and (3) - (5). Here $\gamma_1 = 1.4$ is chosen for the thermodynamic parameter in Equation (3). The density of the pentaerythritol tetranitrate (PETN) used in the experiments was 1440 kg m^{-3}; thus, we use the JWL parameters of ρ_0, A, B, R_1, R_2, and ω for the nearest density (1500 kg m^{-3}) for the PETN detonation products[6] as shown in Table 1. Here, ε_0 is the initial internal energy of the detonation products of PETN, which determines its initial conditions such as pressure. Relationships for the speed of sound in the mixture, c, and in each fluid, c_i, are described in Equation (6).

Table 1 JWL parameters[6] in the present study

ρ_0[kg m^{-3}]	1500
A[GPa]	625.3
B[GPa]	23.29
R_1	5.25
R_2	1.60
ω	0.28
ε_0 [MJ kg^{-1}]	5.71

$$p_1=(\gamma_1-1)\rho_1\varepsilon_1 \tag{3}$$

$$p_2=A\left(1-\frac{\omega}{R_1}\frac{\rho_2}{\rho_0}\right)\exp\left(-R_1\frac{\rho_0}{\rho_2}\right)+B\left(1-\frac{\omega}{R_2}\frac{\rho_2}{\rho_0}\right)\exp\left(-R_2\frac{\rho_0}{\rho_2}\right)+\omega\rho_2\varepsilon_2 \tag{4}$$

$$\begin{cases}\alpha_1+\alpha_2=1\\ \alpha_1\rho_1+\alpha_2\rho_2=\rho\\ \rho_i e_i=\rho_i\varepsilon_i+\dfrac{1}{2}\rho_i(u^2+v^2+w^2)\\ \alpha_1\rho_1 e_1+\alpha_2\rho_2 e_2=\rho e\\ p_1=p_2\end{cases} \tag{5}$$

$$\rho\xi c^2=\textstyle\sum_i \rho_i\alpha_i\xi_i c_i^2,\quad \textit{where},\quad \xi_i=\left(\dfrac{\partial\rho_i\varepsilon_i}{\partial p}\right)_{\rho_i},\quad \xi=\sum\alpha_i\xi_i,$$
$$c_i^2=\left(\frac{\partial p_i}{\partial\rho_i}\right)_{\varepsilon_i}+\frac{p_i}{\rho_i^2}\left(\frac{\partial p_i}{\partial\varepsilon_i}\right)_{\rho_i} \tag{6}$$

In the present study, we use the Harten-Lax-van Leer for Contact scheme[7] to model contact surfaces correctly and maintain accuracy with strong shock waves. We conduct third-order monotone upwind schemes for scalar conservation laws interpolation with a linear scaling limiter[8]. The three-stage total variation diminishing Runge-Kutta method[9] is used for time integration. Figure 1 shows (a) the magazine, cover, and dike models used in the experimental study and (b) the numerically modeled magazine, cover, and dike with the initial position of the high explosive. In this study, the origin is defined at the center of the tube exit on the ground. The center of the high explosive is located 20 mm from the end wall. The detonation products are cylindrical with a diameter of 7.5 mm and a length of 15 mm. In the experiments, the 1-g high explosive comprised 95 wt% PETN and 5 wt% carbon powder. Because the magazine model is symmetric shape, a mirror boundary condition is applied at $y = 0$ mm. We used the immersed boundary-approximated domain method[10] for the walls of the magazine, cover, and dike. A constant grid spacing of 2 mm is set at $-1700\text{mm} \le x \le 2200\text{mm}$, $0\text{mm} \le y \le 1600\text{mm}$, and $0\text{mm} \le z \le 300\text{mm}$. In other regions, the grid spacing is gradually increased, and the full computational domain is $-1700\text{mm} \le x \le 2200\text{mm}$, $0\text{mm} \le y \le 1700\text{mm}$, and $0\text{mm} \le z \le 1700\text{mm}$. To show the azimuthal characteristics on the ground ($z = 0$mm), the azimuth angle θ in the counterclockwise direction is defined from the $+x$ direction as shown in Figure 1b. Here, we should state that the sizes of the magazine, cover, and dike in the experiments and the present simulations do not completely coincide; differences are created by rounding because of the grid spacing of 2 mm.

In addition, we conducted surface explosion calculations on the ground to discuss the enhancement and attenuation of the blast wave by the magazine, cover, and dike. The high explosive was placed vertically, and the height between its center and the steel plate was 18 mm in order to model the experiments.

3. Results

To discuss the azimuthal characteristics on the ground,

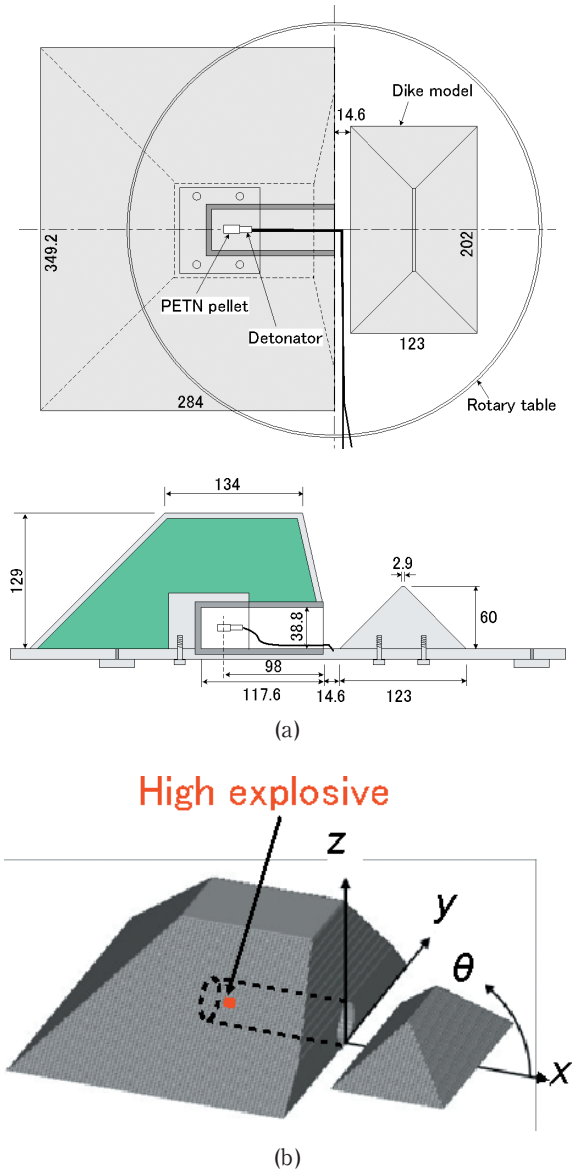

Figure 1 (a) magazine, cover, and dike models used in the experimental study[4]; (b) numerically modeled magazine, cover, and dike with initial position of the high explosive.

we show the flow patterns both with and without a dike. Figure 2 shows the instantaneous flow patterns of density distributions in the $y = 0$ and $z = 0$ planes both (a) without and (b) with a dike. The red surface denotes a detonation-product volume fraction of 0.01, there being higher-concentration detonation products inside the red surface. The shock wave and detonation products exit via the opening.

First, we focus on the difference in detonation-product behavior due to the dike. Without the dike, the blast wave and the detonation products expand smoothly from the exit with pronounced azimuthal characteristics in the $+x$ direction; in Figure 2 a-D, after the blast wave has expanded far away, the detonation products have reached a distance of 700 mm from the exit in the $+x$ direction. In contrast, with the dike, the blast wave is reflected by the rising slope and diffracted by the descending slope; the dike checks the expansion of the detonation products, as shown in Figure 2b-D.

Next, we consider the propagation behavior of the blast wave along the $y = 0$ and $z = 0$ planes. After the blast wave exits, it is diffracted behind the cover. With the dike, the blast wave is reflected and diffracted off the rising and descending slopes, respectively, of the dike. The diffracted and locally curved blast wave off the descending slope is reflected off the ground, resulting in the generation of a triple point at which three shock waves meet: the incident shock, the reflected shock, and the Mach stem, as shown in Figure 2b-A. The blast wave reflected off the rising slope is observed in Figure 2b-B; it catches up with the incident one, which enhances the incident blast wave. Since the cover is symmetrical and has an angular shape as shown in Figure 1, the blast wave in the $+y$, $-y$, and $+z$ directions behind the cover couples in Figures 2a-C and 2b -C and generates two triple points at $y = 0$ and the ground. This indicates that the local geometrical irregularity of the natural terrain is an important factor in estimating the blast-wave strength.

For safety analysis, we focus on the peak overpressures and propagation of the blast wave on the ground. Figure 3 denotes the peak overpressure in the case of an explosion inside the underground magazine both with and without a dike at $\theta = 0°$, and in the case of a surface explosion. The symbols and lines denote data from the experiments and the present numerical simulations, respectively. The calculated peak overpressures clearly agree well with the experimental data. This indicates that the grid resolution is sufficient to accurately calculate the explosion and blast-wave propagation.

As the blast wave expands from the magazine exit, the peak overpressure at 0° becomes larger than that of a surface explosion. The dike prevents the expansion of the blast wave and detonation products along the exit direction and mitigates the peak overpressure near the dike. However, the diffraction effects no longer appear at large scaled distances, and the peak overpressure approaches that without the dike. As previously mentioned by Sugiyama et al.[11], after the blast wave crosses the dike, the locally mitigated curved blast wave reflects off the ground, resulting in the generation of a triple point on the shock front and local-pressure recovery far from the dike. Therefore, blast-wave mitigation by the dike is limited to near the dike, as shown in Figure 3.

To estimate the azimuthal characteristics on the ground, Figure 4 shows the relationship between the azimuth angle θ and the peak overpressure at (a) 400 mm, (b) 800 mm, (c) 1200 mm, and (d) 1600 mm. Again, the symbols and lines denote data from the experiments and the present numerical simulations, respectively. The dashed lines describe the peak overpressure in the case of a surface explosion as calculated by the present simulations (as shown in Figure 3) to show the enhancement and mitigation of the blast wave by the underground magazine. The simulated peak overpressures in Figure 4 agree well with those of the experiments.

Skjeltorp et al.[1] studied the azimuthal characteristics of the blast wave and proposed empirical equations in which

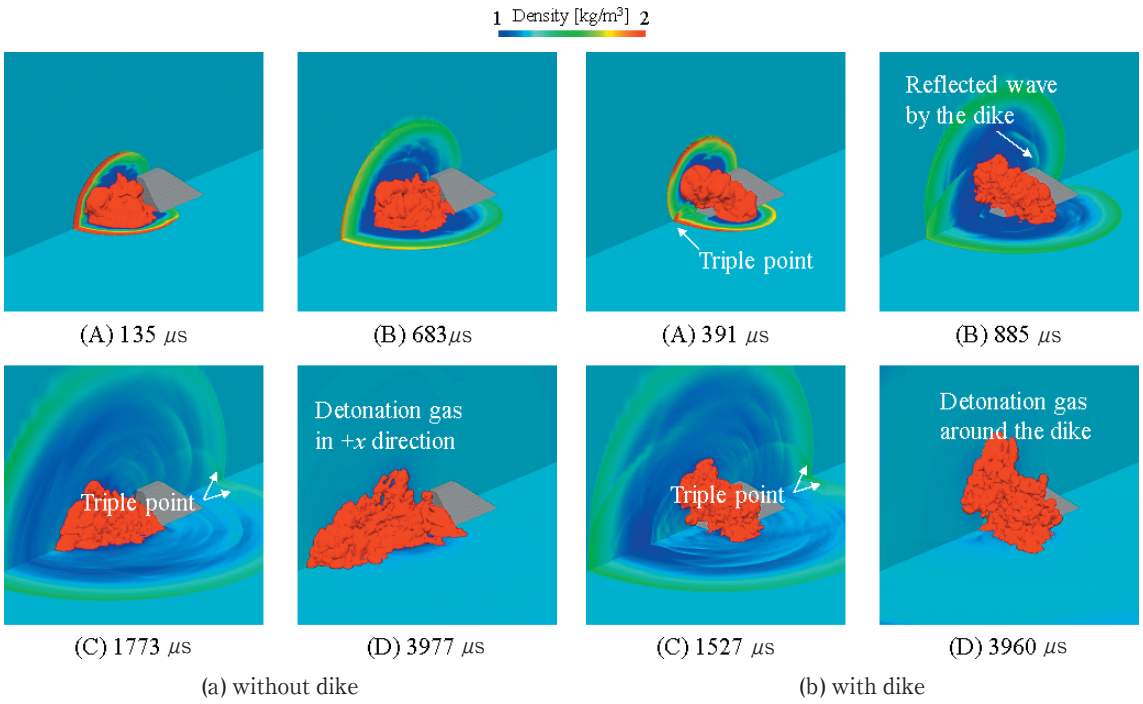

Figure 2 Instantaneous flow patterns of density distributions in the $y = 0$ and $z = 0$ planes: (a) without and (b) with a dike. The red surface denotes detonation-product volume fraction of 0.01.

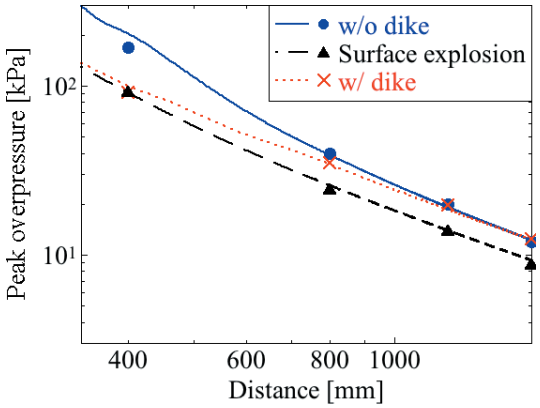

Figure 3 Peak overpressure in the case of explosion inside the underground magazine both with and without dike at $\theta = 0°$, and in the case of a surface explosion. The symbols and lines denote data from the experiments[4] and the present numerical simulations, respectively.

the attenuation index of the peak overpressure versus the scaled distance was constant for all azimuth angles. The empirical equation by Skjeltorp et al.[1] denotes that the increment of the azimuth angle gives a monotonic reduction of the peak overpressure. However, since the reflection and diffraction effects at the dike and the cover create a disturbed blast wave, the different azimuthal characteristics are observed, as mentioned in the previous paper[4].

Regardless of the presence or absence of the dike, the peak overpressures at azimuth angles between 0 and 70° are larger than those of the surface explosion. The diffraction effect by the dike appears at $\theta \leq 60°$ at 400 mm but gradually diminishes, inducing the recovery of the peak overpressure because of the generation of the triple point as shown in Figure 2 b-A. The blast wave reflects off the dike, resulting in it being enhanced for $\theta \geq 60°$ because the reflected wave catches up with the incident blast wave as shown in Figure 2 b-B. The reflection effect continues at large distances, as shown in Figure 4 d. Around 180°, the blast waves from the $+y$, $-y$, and $+z$ directions meet at the $-x$ axis and the superposed blast wave is locally enhanced, as shown in Figures 2 b-C and 4.

In the present study, since numerical simulation can provide much more data than can experiments, the peak overpressure distribution on the ground is discussed to understand the explosion physics from the underground magazine exit. Figure 5 shows schematics of the conversion of the iso-pressure zone from the blast-wave propagation of (a) a surface explosion to (b) an explosion inside the underground magazine. Here, a blue arrow denotes the vertex of the ellipse of the iso-pressure zone in the y direction. In the case of the surface explosion, the blast wave expands hemispherically and hence the iso-pressure zone on the ground becomes a circle whose center is fixed at the ignition point. In contrast, in the case of the explosion inside the underground magazine, the blast wave expands and propagates from the exit in the $+x$ direction. Here, we assume that the blast wave from the underground magazine expands as an ellipsoid and that its center moves in the $+x$ direction. An iso-pressure circle of radius R from the ignition point in the case of the surface explosion becomes an iso-pressure ellipse in the case of the explosion inside the underground magazine, as described by Equation (7) and Figure 5:

$$x^2 + y^2 = R^2 \rightarrow \frac{(x - x_0)^2}{a^2} + \frac{y^2}{b^2} = 1. \quad (7)$$

Here, the parameters describing the ellipse are x_0, a, and b; they are written as functions of R in order to obtain a simple conversion of the iso-pressure region.

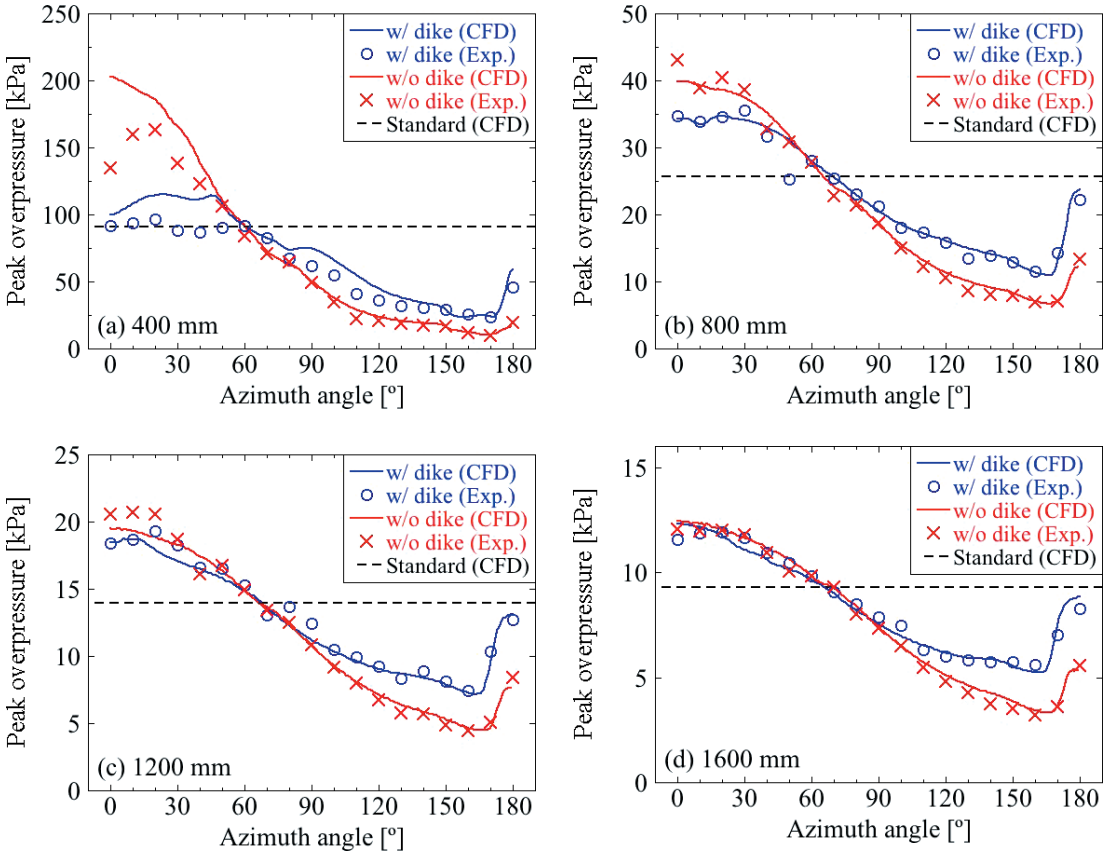

Figure 4 Relationship between azimuth angle θ and peak overpressure at (a) 400 mm, (b) 800 mm, (c) 1200 mm, and (d) 1600 mm. Symbols and solid lines denote data from the previous experiments and the present numerical simulations, respectively. Dashed line describes the peak overpressure in the case of the surface explosion by the present simulation as shown in Figure 3.

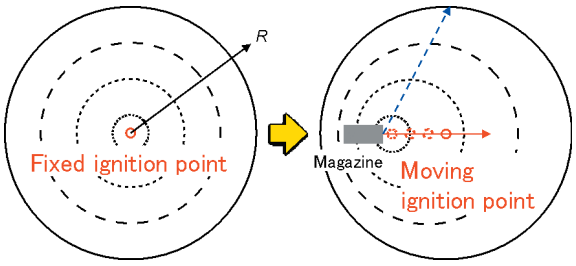

Figure 5 Schematic of the conversion of the iso-pressure zone from the blast-wave propagation of (a) a surface explosion to (b) an explosion inside the underground magazine.

Figure 6 shows the iso-pressure zones and the approximated ellipses. The values of the colored iso-pressure zones are those at $R = 400 - 1600$ mm in 200 mm increments in the case of the surface explosion; the values are described in Figure 3. Our numerical study showed that the iso-pressure zones from the underground magazine would be described as ellipses. As the cover locally enhances the peak overpressure around 180° as shown in Figure 4, the iso-pressure region around 180° cannot be considered and is therefore neglected for describing the ellipses.

Figure 7 shows the relationship between the distance R of the surface explosion and x_0, a, and b in Equation (7) both (a) without and (b) with the dike; x_0, a, and b are described by linear functions of R and have the following properties to note. The intercepts of a and b are at the origin, which confirms that the blast-wave expansion starts from the magazine exit. The gradients of b and x_0 are estimated to be 0.95 and 0.31, respectively, independent of whether or not the dike is present. The absolute gradient of the blast-wave expansion in the y direction, which is described as the blue arrow in Figure 5, assumes a synthesized value of $1.00 = \sqrt{0.95^2 + 0.31^2}$, indicating that the blast-wave expansion of the explosion inside the underground magazine in the y direction corresponds to that of the surface explosion.

In the case without the dike, since the initial strong expansion occurs in the $+x$ direction, the intercept of x_0 becomes larger and the gradient of a becomes smaller than those with the dike. With the dike, the initial strong expansion is constrained to the $+x$ direction, and the intercept of x_0 becomes the origin. The ratio of a and b approaches unity, which corresponds to a circle.

Our study shows that the iso-pressure circle in the case of the surface explosion can become an iso-pressure ellipse in the case of the explosion from the underground magazine. This process could be used to determine the ESQD of an underground magazine. However, in the present study, we do not know whether the properties of x_0, a, and b are universal because of the lack of a parametric study (different sizes and shapes of magazine and dike). Further study will reveal the properties of x_0, a, and b in Equation (7).

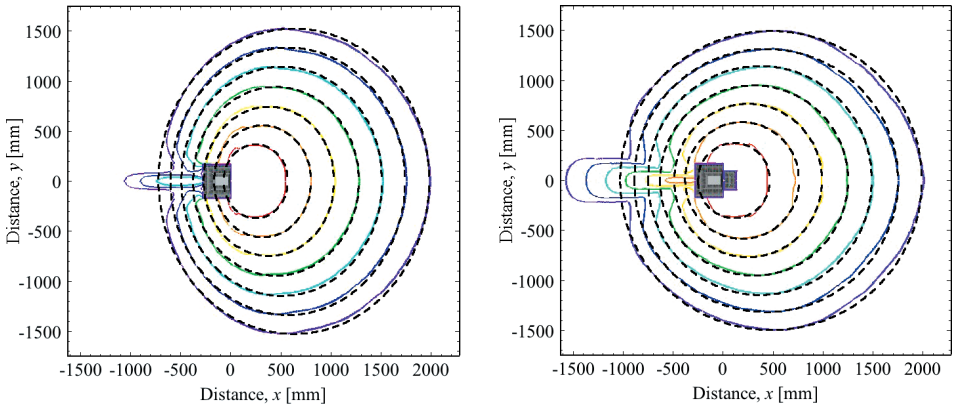

(a) without dike (b) with dike

Figure 6 Iso-pressure zones and their approximated ellipses. The values of the colored iso-pressure zones are those at $R = 400 - 1600$ mm of the surface explosion.

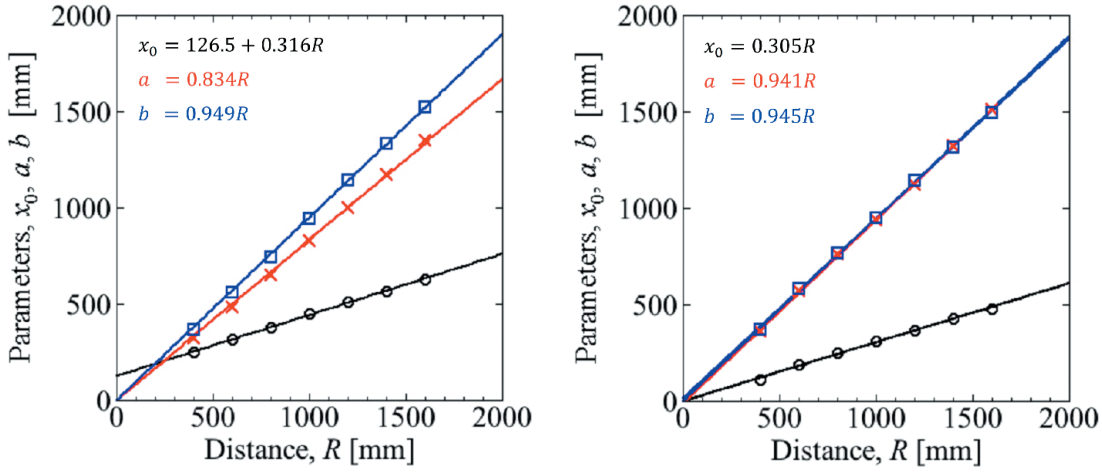

(a) without dike (b) with dike

Figure 7 Relationship between the distance R of the surface explosion and x_0, a, and b in Equation (7): (a) without the dike; (b) with the dike.

4. Conclusion

We modeled the experiments in the previous paper (I) numerically and studied the flow patterns to understand the effects of a dike on an explosion inside an underground magazine. The magazine had an internal length-to-diameter ratio $L/D = 3$. The flow patterns showed that the dike prevents the detonation products from expanding along the exit direction, mitigates the peak overpressure near the dike, and enhances the blast wave behind the magazine through reflection. Our numerical simulations correctly estimated the blast-wave strength as a function of the azimuth angle. Our study showed that the iso-pressure circle in the case of a surface explosion can be converted to an iso-pressure ellipse in the case of an explosion from the underground magazine.

Acknowledgement

This study was made possible by a METI (Ministry of Economy, Trade, and Industry) sponsored project named "technical standard for explosion mitigation of explosives" in FY2015.

References

1) A. T. Skjeltorp, R. Jenssen, and A. Rinnan, Proc. of the Fifth International Symposium on Military Application of Blast Simulators, p. 6 : 7 : 1, Stockholm, May (1977).
2) US Department of Defence, DoD6055.9−STD (2008).
3) L. K. Davis and S.-Y. Song, Joint U. S. / ROK R&D Program for New Underground Ammunition Storage Technologies TR SL−97− 10 and UAST−TR−97−002 (1997).
4) Y. Sugiyama, K. Wakabayashi, T. Matsumura, and Y. Nakayama, Sci. Tech. Energetic Materials, 77, 136−141 (2016).
5) G. Allaire, S. Clerc, and S. Kokh, J. Comput. Phys. 181, 577−616 (2002).
6) E. Lee, M, Finger, and W. Collins, LLNL report, UCID−16189, (1973)
7) E. F. Toro, M. Spruce, and W. Speares, Shock Waves 4, 25−34 (1994).
8) X. Zhang and C. W. Shu, Proc. R. Soc. A 467, 2752−2776 (2011).
9) C. W. Shu and S. Osher, J. Comput. Phys. 77, 439−471 (1988).
10) S. Kang, G. Iaccarino, F. Ham, and P. Moin, J. Comput. Phys. 228, 6753−6772 (2009).
11) Y. Sugiyama, Y. Homae, K. Wakabayashi, T. Matsumura, and Y. Nakayama, Sci. Tech. Energetic Materials, 76, 92−97 (2015).